Transmission electron microscopy studies of the effect of A-site cation size mismatch and disorder on charge ordering behavior in $(La_{1-x}Y_x)_{0.5}(Ca_{1-y}Sr_y)_{0.5}MnO_3$

Y. Q. Wang[a] and X. F. Duan
Beijing Laboratory of Electron Microscopy, Institute of Physics and Center for Condensed Matter Physics, Chinese Academy of Sciences, P.O. Box 2724, Beijing 100080, China

Z. H. Wang and B. G. Shen
State Key Laboratory of Magnetism, Institute of Physics, Center for Condensed Matter Physics, Chinese Academy of Sciences, Beijing 100080, China

(Received 20 November 2000; accepted for publication 16 February 2001)

The effects of A-site cation mismatch and disorder on the charge ordering (CO) behavior in the manganites $(La_{1-x}Y_x)_{0.5}(Ca_{1-y}Sr_y)_{0.5}MnO_3$ have been studied by transmission electron microscopy. The presence of the size mismatch and disorder suppresses the CO transition. Incommensurate CO modulations are observed in three samples with $0 \leqslant \sigma^2 \leqslant 0.003$. Structural models, based on the selected area electron diffraction and high-resolution electron microscopy observation, are suggested for such kinds of incommensurate modulations. © *2001 American Institute of Physics.* [DOI: 10.1063/1.1364505]

In manganese systems, the charge ordering (CO) modulation (resulting from the ionic ordering of Mn^{3+} and Mn^{4+} associated with the d_{z^2} orbital ordering) is induced by the development of a Jahn–Teller distortion of the $Mn^{3+}O_6$ octahedra. In particular, the CO phenomena in the ABO_3-type rare earth manganites with the formula, $Ln_{1-x}A_xMnO_3$, have been the subject of several studies,[1–7] since these are associated with the magnetotransport properties that are sensitive to electronic and geometric factors. It has recently been found that size mismatch and disorder of A-site cations play an important role on the magnetic and transport properties of the manganites.[8,9] In order to explain the effects due to the strain arising from the size mismatch of A-site cations on the Curie temperature T_C, Rodriguez-Martinez *et al.*[8,9] used the variance in the distribution of the average size of A-site cations to quantify the A-site cation size mismatch. The variance is defined by $\sigma^2 = \Sigma x_i r_i^2 - \langle r_A \rangle^2$, where x_i is the fractional occupancy of A site ions and r_i is the corresponding ionic radii. $\langle r_A \rangle$ is the average radius of A-site cations. For $La_{0.5}Ca_{0.5}MnO_3$, $\langle r_A \rangle$ is equal to 1.198 Å. Rodriguez-Martinez and Attfield[8,9] studied the effects of cation mismatch and disorder in the manganites of the type $Re_{0.7}A_{0.3}MnO_3$ for a fixed value of $\langle r_A \rangle$. They found that T_C decreases linearly with increasing σ^2. Fontcuberta *et al.*[10] studied the relationship between the T_C and external pressure in the sample $Ln_{2/3}A_{1/3}MnO_3$ with different $\langle r_A \rangle$ and σ^2. Vanitha *et al.*[11] studied the effect of the cation size disorder on CO in rare-earth manganites (with fixed value of $\langle r_A \rangle$:1.24 and 1.17 Å). They found that the CO transition in the rare-earth manganites was not very sensitive to the size mismatch of the A-site cations or to the orthorhombic lattice distortion arising from the small cation size. For the $(La_{1-x}Y_x)_{0.5}(Ca_{1-y}Sr_y)_{0.5}MnO_3$ (with fixed $\langle r_A \rangle$:1.198 Å) system studied, the measurements of the magnetization-temperature (M–T) curves[12] showed that the CO transition temperature (T_{CO}) evidently decreases with increasing σ^2. So we think it is necessary to study the effect of size mismatch and disorder of A-site cation on the CO transition of the manganites.

In this letter, we report transmission electron microscopy (TEM) studies of the effect of the A-site cation mismatch and disorder on the CO behavior of four compositions with different σ^2 and fixed $\langle r_A \rangle$ in the $(La_{1-x}Y_x)_{0.5}(Ca_{1-y}Sr_y)_{0.5}MnO_3$ system, using the selected area electron diffraction (SAED) and high-resolution electron microscopy (HREM).

Polycrystalline samples $(La_{1-x}Y_x)_{0.5}(Ca_{1-y}Sr_y)_{0.5}MnO_3$ were synthesized by the conventional solid-state reaction from La_2O_3, Y_2O_3, $CaCO_3$, $SrCO_3$, and $MnCO_3$. Four samples with different composition (x,y) were selected for TEM studies. X-ray diffraction patterns[12] for the four samples can be indexed using the orthorhombic crystal structure ($a \approx b = 5.41$ Å, $c = 7.63$ Å). Specimens for transmission electron microscopy studies were prepared by mechanical polishing followed by ion milling. A Philips CM200-FEG transmission electron microscope equipped with low temperature specimen stage and Gatan imaging filter system was used for SAED and HREM studies. All the TEM studies were carried out at liquid nitrogen temperature (93 K).

From measurements of the M–T curves for these samples, it was found that the T_{CO} decreases with increasing σ^2. At $\sigma^2 = 0.005$, the CO transition disappeared, and a spin-glass state appeared. It was concluded that the size mismatch and disorder had a suppression effect on the CO. The σ^2 and initial T_{CO} for the four samples with fixed $\langle r_A \rangle$ value of 1.198 Å and constant Mn^{3+}/Mn^{4+} ratio are listed in the Table I.[12] In order to verify that the Mn^{3+}/Mn^{4+} ratio was constant (equal to 1), electron energy-loss spectroscopy was performed using the ratio of the intensity of white lines to

[a]Electronic mail: yiqianwang@usa.net

 © 2001 American Institute of Physics

TABLE I. The σ^2 and initial T_{CO} of $(La_{1-x}Y_x)_{0.5}(Ca_{1-y}Sr_y)_{0.5}MnO_3$ with fixed $\langle r_A \rangle$ value of 1.198 Å and constant Mn^{3+}/Mn^{4+} ratio. σ^2 was calculated using the following cation radii (see Ref. 13): $\langle r_{La^{3+}} \rangle = 1.216$ Å, $\langle r_{Y^{3+}} \rangle = 1.075$ Å, $\langle r_{Ca^{2+}} \rangle = 1.18$ Å, $\langle r_{Sr^{2+}} \rangle = 1.31$ Å.

Sample name	x	y	σ^2	T_{CO} (K)
CR-0	0	0	0.000	230
CR-1	0.048	0.052	0.001	210
CR-3	0.191	0.207	0.003	160
CR-5	0.333	0.361	0.005	Without

determine the valence state of manganese following the method of Wang *et al.*[14] The results[15] showed that the valence state of manganese was constant (3.5) in all samples.

The SAED patterns recorded at liquid nitrogen temperature from the four samples are shown in Figs. 1(a)–1(d), respectively. Figure 1(a) is a [0 0 1] zone-axis diffraction pattern taken from CR-0 sample. It can be seen clearly that superlattice spots are evident in addition to the fundamental Bragg reflections, which are characterized as the incommensurate modulation due to the CO and orbital ordering. The modulation period is about 11.5 Å; the satellites are not exactly along **a***, but slightly inclined. The wave vector **q** of the superlattice modulation can be written as $\mathbf{q}=(2\pi/\mathbf{a})\times(0.47,\delta_0,0)$. With the substitution of La with Y and Ca with Sr, there is increased size mismatch and disorder in the A-site cations. This is reflected in the [0 3 1] zone-axis diffraction pattern [Fig. 1(b)] recorded from the CR-1 sample. Because of the larger A-site cation size mismatch and disorder in CR-1 sample, the modulation period changes a little from 11.5 to 12.4 Å, compared with Fig. 1(a). Furthermore, the modulation direction has a larger deviation from **a***. The wave vector of this modulation can be written as $\mathbf{q}=(2\pi/\mathbf{a})(0.44,\delta_1,0)$. Figure 1(c) is a [0 0 1] zone-axis diffraction pattern recorded from the CR-3 sample. There are two sets of superlattice spots perpendicular to each other, which are actually originated from 90° twin-related domains. It can be clearly seen from Fig. 1(c) that the superlattice reflections are broadened and become streaked along **a*** [indicated by an arrow in Fig. 1(c)]. The modulation period changes to 14.7 Å, with a wave vector of $\mathbf{q}=(2\pi/\mathbf{a})\times(0.37,\delta_3,0)$. Finally, in the CR-5 sample, having the greatest size mismatch and disorder, there is no evidence of CO, either from the M–T measurement or from the SAED pattern. Figure 1(d) is a [0 0 1] zone-axis diffraction pattern obtained from the CR-5 sample, and no clear modulation reflections are observed. Thus, it is clear that increasing size mismatch and disorder have suppressed the CO transition.

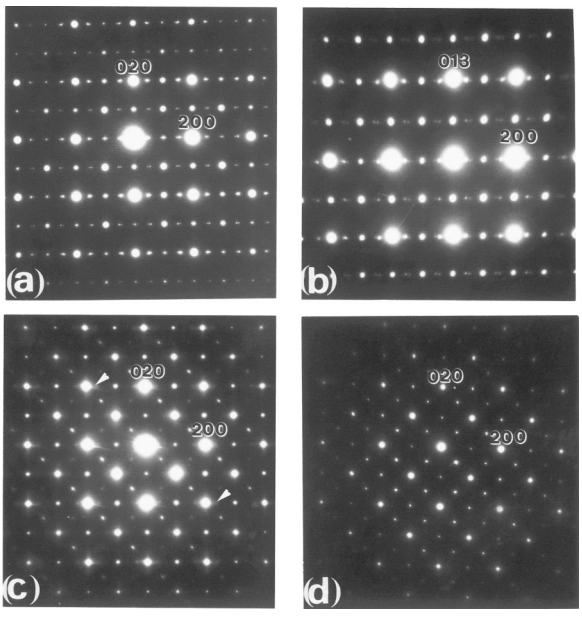

FIG. 1. Selected area diffraction patterns recorded from samples CR-0, CR-1, CR-3, CR-5, all recorded at 93 K.

Generally speaking, there are two basic prerequisites for the formation of CO state: the commensuration of different-charge ions and the Coulombian interaction U between different-charge ions greater than the kinetic energy of electrons E_k. In fact, only when the $\langle r_A \rangle$, which determines the band gap of electrons, is smaller than about 1.25 Å,[16] can the CO transition take place in the $Ln_{0.5}A_{0.5}MnO_3$. In addition to this dependence on $\langle r_A \rangle$, however, increasing the size mismatch and disorder of A-site cations suppresses the CO transition. Maignan *et al.*[17] studied the magnetic and transport properties of $Ln_{0.5}Ca_{0.5}MnO_3$(Ln=Pr, Nd, Sm) by substitution of Mn with Ni, and it was found that a small amount of Ni would destroy the CO state. In the $Pr_{0.5}Ca_{0.5}MnO_3$ system using the substitution of Mn with Cr, Damay *et al.*[18] observed similar phenomena. The incommensurate modulations found in the $Nd_{0.5}Ca_{0.5}Mn_{1-x}Cr_xO_3$[19] system were explained by the presence of a slight excess of $Mn^{4+}(Mn^{4+}/Mn^{3+}>1)$. In summary, in those studies, the suppression effect on the CO state by the substitution of Mn was attributed to the destruction of the commensurate ratio of Mn^{4+} and Mn^{3+}. However, the Mn^{3+}/Mn^{4+} ratios in all four samples in this study were constant and very close to 1. The suppression effect of the size mismatch and disorder can, therefore, not simply be explained by the presence of excess $Mn^{4+}(Mn^{4+}/Mn^{3+}>1)$ or excess $Mn^{3+}(Mn^{4+}/Mn^{3+}<1)$.

To clarify the nature of the incommensurate modulations, the HREM technique was used. Figure 2 is a [0 0 1] zone-axis HREM image recorded from CR-0 sample at 93 K. The regions (a) and (b) are enlarged later. There are three distinct features in this image that can explain the incommensurate modulation observed in the SAED pattern.

(1) The first phenomenon deals with the fact that the number of adjacent 1:1 ordered cells ($2a_p\sqrt{2}$) is not always perfectly regular, exactly like in intergrowths. Moreover, one sometimes observes that the local sequences consist of n adjacent ordered cells separated by one defective adjacent simple cell [residual discommensurations can be seen in region (a)]. The local fringe periodicity is then 16.3 Å($3a_p\sqrt{2}$). So the original periodicity ($2a_p\sqrt{2}$) is changed due to the larger discommensurations. This can explain why the periodicity of the incommensurate modulation is a little larger [11.5 Å determined by the SAED pattern in Fig. 1(a)] than $2a_p\sqrt{2}$.

(2) The second phenomenon corresponds to the shifting of the fringes along **a**. The amplitude of the translation along **a** is $a_p\sqrt{2}$ or $a_p\sqrt{2}/2$. Note that the formation of such areas implies that the modulation vector is no longer parallel to **a**, but that it involves components along **a** and **c**. This is the

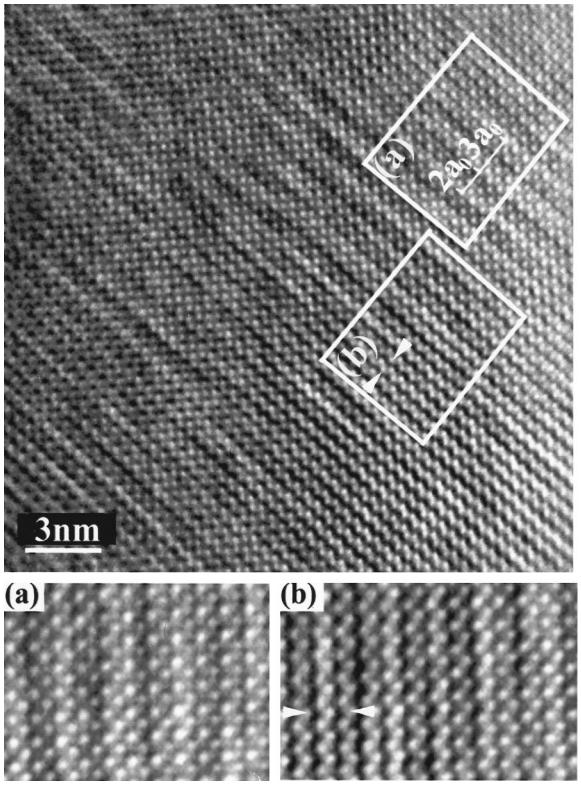

FIG. 2. The [0 0 1] zone-axis HREM image of CR-0 sample obtained at 93 K.

reason that the modulation direction [in Fig. 1(a)] is not exactly along **a**, with a small deviation.

(3) In region (b), there exists antiphase boundaries (highlighted by two arrows). The phase difference on either side of the antiphase boundary is π. That is also to say, the bright fringe is locally connected to a gray one. The periodicity of modulation is not changed. This can be explained through the model proposed by Mori *et al.*[20]

Based on the SAED and HREM observation, structural models (after Barnabé *et al.*)[21] for the evolution of CO behaviors in the four samples are shown in Fig. 3. Although the size mismatch and disorder do not affect the ratio of Mn^{3+} and Mn^{4+} in all the samples, the structures [Figs. 3(a), 3(b), and 3(c)] of the incommensurate crystals could consist of regions with additional $[Mn^{4+}]$ layers and regions with some Mn^{3+} species distributed in the $[Mn^{4+}]$ layers. The periodicities of the structural models [Figs. 3(a), 3(b), and 3(c)] for the incommensurate modulated structures in CR-0, CR-1, and CR-3 are in good agreements with those calculated from diffraction patterns in Figs. 1(a), 1(b), and 1(c). From the evolution of the CO behaviors in Fig. 3, it can be clearly seen that the CO and orbital ordering are destroyed gradually. With the greater substitution of La and Ca with Y and Sr, the original CO and orbital ordering will be destroyed gradually, and they will disappear at last (in CR-5 sample with largest size mismatch of $\sigma^2=0.005$). So it is reasonable not to observe the CO transition in the CR-5 sample.

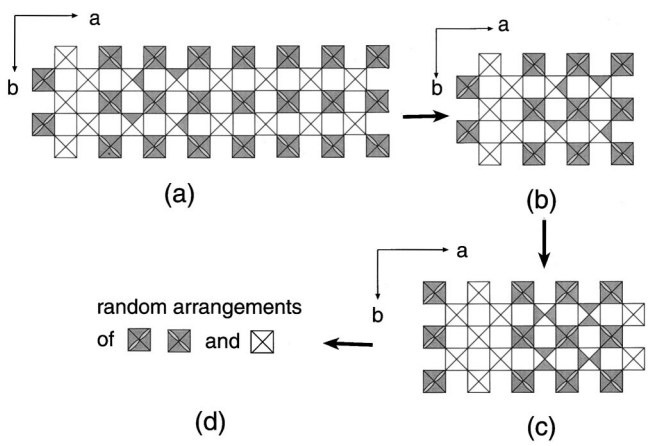

FIG. 3. Schematic models for the evolution of the charge-ordering behaviors in CR-0, CR-1, CR-3, CR-5 samples. ⊠ ⊠ and ⊠ represent Mn^{3+}, Mn^{3+}, and Mn^{4+}, respectively.

In conclusion, the present study indicated that the size mismatch and disorder of A-site cations could suppress the CO transition. Incommensurate CO modulations were observed in three samples (CR-0, 1, 3) of the system $(La_{1-x}Y_x)_{0.5}(Ca_{1-y}Sr_y)_{0.5}MnO_3$. Structural models, based on the SAED and HREM observation, were proposed for such kinds of incommensurate modulations.

The authors would like to thank the support of China NSF outstanding Young Scientist Grant (B-class, No. 59825503), and thank Professor K. H. Kuo for encouragement.

[1] Y. Tomioka, A. Asamitsu, Y. Moritomo, H. Kuwahara, and Y. Tokura, Phys. Rev. Lett. **74**, 5108 (1995).
[2] V. Kiryukhin, D. Casa, J. P. Hill, B. Keimer, A. Vigliante, and Y. Tokura, Nature (London) **386**, 813 (1997).
[3] Y. Moritomo, H. Kuwahara, Y. Tomioka, and Y. Tokura, Phys. Rev. B **55**, 7549 (1997).
[4] A. P. Ramirez, P. Schiffer, S.-W. Cheong, C. H. Chen, W. Bao, T. T. M. Palstra, P. L. Gammel, D. J. Bishop, and B. Zegarski, Phys. Rev. Lett. **76**, 3188 (1996).
[5] C. H. Chen, S.-W. Cheong, and H. Y. Hwang, J. Appl. Phys. **81**, 4326 (1997).
[6] C. H. Chen and S.-W. Cheong, Phys. Rev. Lett. **76**, 4042 (1996).
[7] S. Mori, C. H. Chen, and S. W. Cheong, Nature (London) **392**, 473 (1998).
[8] L. M. Rodriguez-Martinez and J. P. Attfield, Phys. Rev. B **54**, R15622 (1996).
[9] L. M. Rodriguez-Martinez and J. P. Attfield, Phys. Rev. B **58**, 2426 (1998).
[10] J. Fontcuberta, V. Laukhin, and X. Obradors, Appl. Phys. Lett. **72**, 2607 (1998).
[11] P. V. Vanitha, P. N. Santhosh, R. S. Singh, C. N. R. Rao, and J. P. Attfield, Phys. Rev. B **59**, 13 539 (1999).
[12] Z. H. Wang, Ph.D thesis, Institute of Physics, Chinese Academy of Sciences, China, 1999.
[13] R. D. Shannon, Acta Crystallogr., Sect. A: Cryst. Phys., Diffr., Theor. Gen. Crystallogr. **32**, 751 (1976).
[14] Z. L. Wang, J. S. Yin, and Y. D. Jiang, Micron **31**, 571 (2000).
[15] Y. Q. Wang, I. Maclaren, and X. F. Duan, Mater. Sci. Eng., A (to be published).
[16] C. N. R. Rao, R. Mahesh, A. K. Raychaudhuri, and R. Mahendiran, J. Phys. Chem. Solids **59**, 487 (1998).
[17] A. Maignan, F. Damay, C. Martin, and B. Raveau, Mater. Res. Bull. **32**, 965 (1997).
[18] F. Damay, C. Martin, A. Maignan, M. Hervieu, B. Raveau, F. Bourée, and G. André, Appl. Phys. Lett. **73**, 3772 (1998).
[19] W. Schuddinck, G. Van Tendeloo, A. Barnabé, M. Hervieu, and B. Raveau, J. Magn. Magn. Mater. **211**, 105 (2000).
[20] S. Mori, C. H. Chen, and S.-W. Cheong, Phys. Rev. Lett. **81**, 3972 (1998).
[21] A. Barnabé, M. Hervieu, C. Martin, A. Maignan, and B. Raveau, J. Appl. Phys. **84**, 5506 (1998).